applied sciences

MDPI

Article

FDTD Method for Electromagnetic Simulations in Media Described by Time-Fractional Constitutive Relations

Piotr Pietruszka [1], Tomasz P. Stefański [1] and Jacek Gulgowski [2,*]

[1] Faculty of Electronics, Telecommunications and Informatics, Gdansk University of Technology, 80-233 Gdansk, Poland; piotr.parsley@gmail.com (P.P.); tomasz.stefanski@pg.edu.pl (T.P.S.)
[2] Faculty of Mathematics, Physics and Informatics, University of Gdansk, 80-308 Gdansk, Poland
* Correspondence: jacek.gulgowski@ug.edu.pl

Abstract: In this paper, the finite-difference time-domain (FDTD) method is derived for electromagnetic simulations in media described by the time-fractional (TF) constitutive relations. TF Maxwell's equations are derived based on these constitutive relations and the Grünwald–Letnikov definition of a fractional derivative. Then the FDTD algorithm, which includes memory effects and energy dissipation of the considered media, is introduced. Finally, one-dimensional signal propagation in such electromagnetic media is considered. The proposed FDTD method is derived based on a discrete approximation of the Grünwald–Letnikov definition of the fractional derivative and evaluated in a code. The stability condition is derived for the proposed FDTD method based on a numerical-dispersion relation. The obtained numerical results are compared with the outcomes of reference frequency-domain simulations, proving the accuracy of the proposed approach. However, high spatial resolution is required in order to obtain accurate results. The developed FDTD method is, unfortunately, computation and memory demanding when compared to the ordinary FDTD algorithm.

Keywords: finite-difference time-domain; fractional calculus; Grünwald–Letnikov derivative; Maxwell's equations; stability limit

Citation: Pietruszka, P.; Stefański, T.P.; Gulgowski, J. FDTD Method for Electromagnetic Simulations in Media Described by Time-Fractional Constitutive Relations. *Appl. Sci.* **2023**, *13*, 10654. https://doi.org/10.3390/app131910654

Academic Editor: Giuseppe Lacidogna

Received: 25 July 2023
Revised: 19 September 2023
Accepted: 20 September 2023
Published: 25 September 2023

1. Introduction

Fractional calculus has been used in modeling of electromagnetic phenomena for many years. In particular, time-fractional (TF) derivatives allow for modeling materials with memory effects and energy dissipation [1]. Nonlocality is a crucial property of fractional-order (FO) operators as it allows for including the effects of the electromagnetic-field history on the current response of the media [2]. Notably, the FO models of dielectric media, such as the Cole–Cole or Davidson models, can be used to describe some biological tissues more accurately and over a broader frequency range than the integer-order (IO) ones, e.g., the Debye model [3]. Fractional derivatives can also be applied in modeling of capacitors, which has been experimentally confirmed to be more accurate than the IO classical approach [4,5]. Spatial fractional derivatives, in the form of a fractional curl operator [6], are applied to the description of chiral media [7]. Another possible application of the FO calculus is the formulation of fractional multipoles, which has proved to be useful in solving some electrostatic problems, especially those including perfectly conducting wedges and cones [8].

The finite-difference time-domain (FDTD) method [9] remains one of the most popular techniques of electromagnetic simulation, which is successfully applied to FO models of media. For the Debye, Drude and Lorentz media, whose relative complex permittivity is described by a rational function involving integer powers of $j\omega$, the time-domain expression of the constitutive relation can easily be formulated and implemented inside the FDTD algorithm [10]. On the other hand, the dielectric response involving non-integer powers of

$j\omega$ requires implementation of fractional derivatives in the time domain, which introduces difficulties in terms of domain discretization and computational overhead. In the early approach [11,12], dielectrics with fractional relaxation of the Cole–Cole, Cole–Davidson and Havriliak–Negami models are implemented based on approximation of the dielectric response by the Debye functions. Unfortunately, this technique does not correctly represent the singularity of time-domain susceptibility, which arises from dielectric models with fractional relaxation [13]. Hence, it is not possible, with the use of this technique, to accurately compute the impulse or step response of spatially complex dispersive scatterers. Other approaches employ the Z-transformation for implementation of the Cole–Cole, Cole–Davidson and Havriliak–Negami models of dispersive media. The method based on the Z-transformation and a second-order Taylor approximation of the Cole—Cole formula is proposed in [14]. This approach is then applied to the problem of the penetration of a short electromagnetic pulse into biological matter. The algorithm of the Cole–Cole model implementation in FDTD [15] is developed based on the Z-transformation and the bilinear transformation. The FO differentiators in this model are approximated by polynomials, whose coefficients are found using a least-squares fitting method. In the approach [16], fractional derivatives in the time-domain representation of the dielectric response are circumvented by the use of fast inverse Laplace transformation and Prony's method. The Laplace transformation is used to transform the frequency-domain response of a medium into the time domain, and Prony's method is employed to extract the parameters and transform further the time-domain response into the Z-domain in order to incorporate it directly into the FDTD method. The obtained numerical results are found to be in good agreement with those obtained by an analytical method over a broad frequency range, demonstrating the validity of this FDTD scheme. In other approaches [17,18], the FDTD simulations of the Cole–Cole media employing the auxiliary differential equation (ADE) are proposed. Whilst the former approach [17] approximates the FO differentiation with the use of a rational function derived based on the Padé approximation, the latter approach [18] approximates the FO derivatives linearly between time-steps. Both techniques, therefore, provide efficient ADE schemes with straightforward implementation within the FDTD algorithm. In the approach [19], FDTD is successfully applied to the more general Raicu medium. The proposed method solves Maxwell's equations directly in the time domain with the use of a Riemann–Liouville FO derivative. The obtained results prove the accuracy of this technique in the ultra-wideband frequency range. In [20], a general FDTD scheme, able to incorporate the model of the medium based on the general fractional polynomial series approximation, is presented. Its applicability is further considered in several examples demonstrating its usefulness for understanding a variety of electromagnetic phenomena involving media with power-law frequency dispersion.

The aim of this paper is to present the FDTD method for simulation of wave propagation in the media described by the TF constitutive relations [21]. The considered medium is analysed based on TF Maxwell's equations. In [22], an analysis of Poynting's vector and propagation velocity in such a medium is performed. The causality for a plane wave propagating in the considered medium is confirmed by verification of the Kramers–Krönig relations. In [23], the uniqueness of solutions and the reciprocity are proved. In both papers, the analysis is supported by the results of numerical simulations. These are performed using the frequency-domain simulation method, employing the Fourier and Hilbert transformations, or using the time-domain method, which is based on Green's function computations. In this paper, we investigate an alternative simulation method in an attempt to replicate the existing results and evaluate the applicability of FDTD for the considered media with the TF constitutive relations. The novelty of the paper relies on formulation of FDTD for TF Maxwell's equations, and its evaluation in a code. Furthermore, the stability condition is derived for the proposed FDTD method based on a numerical-dispersion relation.

The paper begins with a short introduction to the fractional-derivative definition and its approximation used throughout the paper. In Section 3, TF Maxwell's equations are derived based on the TF constitutive relations. In Section 4, the FDTD method is

formulated for the media described by the TF constitutive relations, and its stability analysis is performed. Long derivations of dispersion relations and stability conditions are collected in Appendices A–C. In Section 5, the obtained numerical results are presented in reference to the existing frequency-domain method presented in the literature. In Section 6, an analysis of the computational complexity of the developed method is performed. Finally, the conclusions are drawn in Section 7.

2. Fractional Derivative

Let us consider a fractional derivative of the time-variable function $f(t)$, where $f : \mathbb{R} \to \mathbb{R}$. There are many definitions of a fractional derivative, which are not equivalent in the general case [24]. The most prominent ones include the Riemann–Liouville, Caputo, Marchaud and Grünwald–Letnikov definitions. For modeling electromagnetic systems, it is desirable to choose the definition which reflects certain properties, like the semigroup property

$$D_t^{\alpha} D_t^{\beta} f(t) = D_t^{\beta} D_t^{\alpha} f(t) = D_t^{\alpha+\beta} f(t) \tag{1}$$

and the trigonometric function invariance (derivative of the complex exponent)

$$D_t^{\alpha} e^{\Omega t} = \Omega^{\alpha} e^{\Omega t}. \tag{2}$$

In (1) and (2), D_t^{α} denotes the α-order fractional derivative, $\alpha, \beta \in \mathbb{R}$ and $\Omega \in \mathbb{C}$ [25]. The Riemann–Liouville and Caputo definitions do not meet the conditions (1) and (2). The Grünwald–Letnikov and Marchaud definitions, however, satisfy both properties, making them more appropriate for applications in the electromagnetic theory [25]. In this paper, we employ the Grünwald–Letnikov definition given by [2]

$$D_t^{\alpha} f(t) = \lim_{h \to 0^+} \left(\frac{1}{h}\right)^{\alpha} \sum_{l=0}^{\infty} (-1)^l \binom{\alpha}{l} f(t - lh). \tag{3}$$

In the above formula, the symbol $\binom{\alpha}{l}$ for non-integer α is given by

$$\binom{\alpha}{l} = \frac{\alpha(\alpha-1)(\alpha-2)\ldots(\alpha-l+1)}{l!}. \tag{4}$$

Apart from satisfying the desired conditions, the Grünwald–Letnikov definition can also be naturally approximated using finite differences. It is also consistent with the Marchaud definition used by us in previous investigations [22].

The approximation scheme for the derivative $D_t^{\alpha} f(t)$ is natural for a sufficiently small time-step size $T > 0$, and is given by the infinite series

$$D_t^{\alpha} f(t) \approx \left(\frac{1}{T}\right)^{\alpha} \sum_{l=0}^{\infty} (-1)^l \binom{\alpha}{l} f(t - lT). \tag{5}$$

In the case of causal functions (i.e., vanishing for times $t < 0$), it naturally simplifies to the finite sum

$$D_t^{\alpha} f(nT) \approx \left(\frac{1}{T}\right)^{\alpha} \sum_{l=0}^{n} (-1)^l \binom{\alpha}{l} f((n-l)T) \tag{6}$$

when calculated for $t = nT$.

3. FO Model of Dielectric Media

In a homogeneous and isotropic medium, the electromagnetic field satisfies Maxwell's equations

$$\nabla \cdot \mathbf{D} = \rho \tag{7}$$

$$\nabla \times \mathbf{E} = -\frac{\partial \mathbf{B}}{\partial t} \tag{8}$$

$$\nabla \cdot \mathbf{B} = 0 \tag{9}$$

$$\nabla \times \mathbf{H} = \mathbf{J} + \frac{\partial \mathbf{D}}{\partial t} \tag{10}$$

where $\mathbf{D}$ and $\mathbf{B}$ are, respectively, the electric- and magnetic-flux densities, $\mathbf{E}$ and $\mathbf{H}$ are, respectively, the electric- and magnetic-field intensities, $\mathbf{J}$ is the current density and ρ is the volume-charge density.

Let us consider the electromagnetic medium described by the FO constitutive relations

$$\varepsilon_\beta \mathbf{E} = D_t^{1-\beta}\mathbf{D} \tag{11}$$

$$\mu_\gamma \mathbf{H} = D_t^{1-\gamma}\mathbf{B} \tag{12}$$

$$\mathbf{J} = \sigma_\eta D_t^{1-\eta}\mathbf{E} \tag{13}$$

where ε_β, μ_γ, σ_η ($\beta, \gamma, \eta \in (0, 1]$) are parameters corresponding to the permittivity, permeability and conductivity, with units $\frac{\mathrm{F}}{\mathrm{s}^{1-\beta}\mathrm{m}}$, $\frac{\mathrm{H}}{\mathrm{s}^{1-\gamma}\mathrm{m}}$ and $\frac{\mathrm{S}}{\mathrm{s}^{\eta-1}\mathrm{m}}$ (F—Farad, H—Henr, S—Siemens), respectively. Assuming there is no energy dissipation due to Joule heating ($\sigma_\eta = 0$), we can write the set of constitutive relations in the form

$$\varepsilon_\beta D_t^\beta \mathbf{E} = \frac{\partial \mathbf{D}}{\partial t} \tag{14}$$

$$\mu_\gamma D_t^\gamma \mathbf{H} = \frac{\partial \mathbf{B}}{\partial t}. \tag{15}$$

Using (14) and (15), one obtains from (7)–(10) Maxwell's equations with the TF derivatives as follows:

$$\nabla \cdot \mathbf{E} = 0 \tag{16}$$

$$\nabla \times \mathbf{E} = -\mu_\gamma D_t^\gamma \mathbf{H} \tag{17}$$

$$\nabla \cdot \mathbf{H} = 0 \tag{18}$$

$$\nabla \times \mathbf{H} = \varepsilon_\beta D_t^\beta \mathbf{E}. \tag{19}$$

Let us calculate the curl of (17). Then, one obtains

$$\nabla \times \nabla \times \mathbf{E} = -\mu_\gamma \varepsilon_\beta D_t^{\beta+\gamma}\mathbf{E}. \tag{20}$$

Using the vector calculus identity $\nabla \times \nabla \times \mathbf{E} = \nabla(\nabla \cdot \mathbf{E}) - \nabla^2\mathbf{E}$ and (16), one obtains from (20) the fractional diffusion-wave equation for the electric field

$$\nabla^2\mathbf{E} - \mu_\gamma \varepsilon_\beta D_t^{\beta+\gamma}\mathbf{E} = \mathbf{0}. \tag{21}$$

The fractional diffusion-wave equation interpolates between the diffusion and the wave processes, which are completely different with regard to their response to a localized disturbance [22]. That is, the diffusion equation describes a process in which a disturbance spreads infinitely fast, whereas the wave equation describes a process in which a disturbance propagates with a constant finite velocity. For the fractional diffusion-wave equation,

a disturbance spreads with an infinite velocity, but its fundamental solution possesses a maximum which propagates with a finite velocity [26].

Of course, a detailed formulation of the problem in electromagnetics requires not only the Equation (21), but also boundary and initial conditions. While the boundary conditions result from the assumed behavior of the electromagnetic field on the boundary of the spatial domain, the initial conditions are assumed to be a zero electromagnetic field for $t < 0$. For the electromagnetic system described by (16)–(19), employing the Grünwald–Letnikov derivative with an infinite memory of the past, it is important how the current state of the system was obtained. Therefore, the only option is to assume the zero initial conditions, which allow for including the entire history of earlier events in calculations of the current state.

Let us now focus our analysis on the one-dimensional case of a wave propagating along the z-axis, E_x being the electric field, and H_y being the magnetic field. Equations (17) and (19) can then be simplified to

$$\frac{\partial E_x}{\partial z} = -\mu_\gamma D_t^\gamma H_y \tag{22}$$

$$-\frac{\partial H_y}{\partial z} = \varepsilon_\beta D_t^\beta E_x \tag{23}$$

whereas (21) simplifies to

$$\frac{\partial^2 E_x}{\partial z^2} - \mu_\gamma \varepsilon_\beta D_t^{\beta+\gamma} E_x = 0. \tag{24}$$

Let us further assume that $\beta = \gamma = \alpha \in (0.5, 1)$, which means that the cases intermediate between diffusion and wave propagation are considered. This assumption and consideration of the one-dimensional propagation allow us to easily refer to the results generated by the method already presented in the literature.

4. FDTD Algorithm

In this section, the FDTD method for the media described by the TF constitutive relations is presented.

4.1. Update Equations

The FDTD method is based on a leapfrog time-stepping scheme with update equations for the electric and magnetic fields derived from discretized Maxwell's equations [9]. Below, for any discretized function $F : \mathbb{R}^4 \to \mathbb{R}$ representing one of the components E_x, E_y, E_z, H_x, H_y, H_z, we denote

$$F^N(I, J, K) = F(I \cdot \Delta x, J \cdot \Delta y, K \cdot \Delta z, N \cdot \Delta t)$$

where Δt is the time-step size and Δx, Δy, Δz are the spatial-step sizes along the x, y and z directions, respectively. After approximating in (17) and (19) the spatial derivatives by central differences [9] and the TF derivatives by the finite sum (6) (under the assumption $\beta = \gamma = \alpha$), one obtains the following relations, which are used to compute new values of the electric and magnetic fields

$$\begin{aligned} H_x^{n+\frac{1}{2}}(i, j+\frac{1}{2}, k+\frac{1}{2}) = &-\sum_{l=1}^{n} w_l^\alpha H_x^{n-l+\frac{1}{2}}(i, j+\frac{1}{2}, k+\frac{1}{2}) + \\ &\frac{(\Delta t)^\alpha}{\mu_\alpha}\left(\frac{E_y^n(i, j+\frac{1}{2}, k+1) - E_y^n(i, j+\frac{1}{2}, k)}{\Delta z} - \right. \\ &\left. \frac{E_z^n(i, j+1, k+\frac{1}{2}) - E_z^n(i, j, k+\frac{1}{2})}{\Delta y}\right) \end{aligned} \tag{25}$$

$$H_y^{n+\frac{1}{2}}(i+\frac{1}{2},j,k+\frac{1}{2}) = -\sum_{l=1}^{n} w_l^{\alpha} H_y^{n-l+\frac{1}{2}}(i+\frac{1}{2},j,k+\frac{1}{2}) + \frac{(\Delta t)^{\alpha}}{\mu_{\alpha}}\left(\frac{E_z^n(i+1,j,k+\frac{1}{2}) - E_z^n(i,j,k+\frac{1}{2})}{\Delta x} - \frac{E_x^n(i+\frac{1}{2},j,k+1) - E_x^n(i+\frac{1}{2},j,k)}{\Delta z}\right) \tag{26}$$

$$H_z^{n+\frac{1}{2}}(i+\frac{1}{2},j+\frac{1}{2},k) = -\sum_{l=1}^{n} w_l^{\alpha} H_z^{n-l+\frac{1}{2}}(i+\frac{1}{2},j+\frac{1}{2},k) + \frac{(\Delta t)^{\alpha}}{\mu_{\alpha}}\left(\frac{E_x^n(i+\frac{1}{2},j+1,k) - E_x^n(i+\frac{1}{2},j,k)}{\Delta y} - \frac{E_y^n(i+1,j+\frac{1}{2},k) - E_y^n(i,j+\frac{1}{2},k)}{\Delta x}\right) \tag{27}$$

$$E_x^{n+1}(i+\frac{1}{2},j,k) = -\sum_{l=1}^{n} w_l^{\alpha} E_x^{n-l+1}(i+\frac{1}{2},j,k) + \frac{(\Delta t)^{\alpha}}{\varepsilon_{\alpha}}\left(\frac{H_z^{n+\frac{1}{2}}(i+\frac{1}{2},j+\frac{1}{2},k) - H_z^{n+\frac{1}{2}}(i+\frac{1}{2},j-\frac{1}{2},k)}{\Delta y} - \frac{H_y^{n+\frac{1}{2}}(i+\frac{1}{2},j,k+\frac{1}{2}) - H_y^{n+\frac{1}{2}}(i+\frac{1}{2},j+\frac{1}{2},k-\frac{1}{2})}{\Delta z}\right) \tag{28}$$

$$E_y^{n+1}(i,j+\frac{1}{2},k) = -\sum_{l=1}^{n} w_l^{\alpha} E_y^{n-l+1}(i,j+\frac{1}{2},k) + \frac{(\Delta t)^{\alpha}}{\varepsilon_{\alpha}}\left(\frac{H_x^{n+\frac{1}{2}}(i,j+\frac{1}{2},k+\frac{1}{2}) - H_x^{n+\frac{1}{2}}(i,j+\frac{1}{2},k-\frac{1}{2})}{\Delta z} - \frac{H_z^{n+\frac{1}{2}}(i+\frac{1}{2},j+\frac{1}{2},k) - H_z^{n+\frac{1}{2}}(i-\frac{1}{2},j+\frac{1}{2},k)}{\Delta x}\right) \tag{29}$$

$$E_z^{n+1}(i,j,k+\frac{1}{2}) = -\sum_{l=1}^{n} w_l^{\alpha} E_z^{n-l+1}(i,j,k+\frac{1}{2}) + \frac{(\Delta t)^{\alpha}}{\varepsilon_{\alpha}}\left(\frac{H_y^{n+\frac{1}{2}}(i+\frac{1}{2},j,k+\frac{1}{2}) - H_y^{n+\frac{1}{2}}(i-\frac{1}{2},j,k+\frac{1}{2})}{\Delta x} - \frac{H_x^{n+\frac{1}{2}}(i,j+\frac{1}{2},k+\frac{1}{2}) - H_x^{n+\frac{1}{2}}(i,j-\frac{1}{2},k+\frac{1}{2})}{\Delta y}\right). \tag{30}$$

The coefficients of the Grünwald–Letnikov derivative $w_l^{\alpha} = (-1)^l \binom{\alpha}{l}$ can be computed in a recursive manner, which allows for reducing the computational overhead as follows:

$$w_l^{\alpha} = \left(1 - \frac{1+\alpha}{l}\right) w_{l-1}^{\alpha}, \quad w_0^{\alpha} = 1. \tag{31}$$

This relation holds true because

$$w_l^{\alpha} = (-1)^l \binom{\alpha}{l} = (-1)^l \frac{\alpha(\alpha-1)(\alpha-2)\ldots(\alpha-l+1)}{l!} = \tag{32}$$

$$(-1)\cdot(-1)^{l-1}\frac{\alpha(\alpha-1)(\alpha-2)\ldots(\alpha-l+2)}{(l-1)!}\frac{\alpha-l+1}{l}=\left(1-\frac{\alpha+1}{l}\right)w_{l-1}^{\alpha}.$$

In the one-dimensional case, the update equations simplify to

$$H_y^{n+\frac{1}{2}}\left(k+\frac{1}{2}\right)=-\sum_{l=1}^{n}w_l^{\alpha}H_y^{n-l+\frac{1}{2}}\left(k+\frac{1}{2}\right)-\frac{(\Delta t)^{\alpha}}{\mu_{\alpha}}\frac{E_x^n(k+1)-E_x^n(k)}{\Delta z} \tag{33}$$

$$E_x^{n+1}(k)=-\sum_{l=1}^{n}w_l^{\alpha}E_x^{n+1-l}(k)-\frac{(\Delta t)^{\alpha}}{\varepsilon_{\alpha}}\frac{H_y^{n+\frac{1}{2}}\left(k+\frac{1}{2}\right)-H_y^{n+\frac{1}{2}}\left(k-\frac{1}{2}\right)}{\Delta z}. \tag{34}$$

4.2. Stability

In the IO case of the FDTD method ($\alpha=1$), the time-step size is limited by the Courant condition [9]

$$\Delta t\le\frac{1}{c_0\sqrt{\frac{1}{(\Delta x)^2}+\frac{1}{(\Delta y)^2}+\frac{1}{(\Delta z)^2}}} \tag{35}$$

where c_0 denotes the light speed in a vacuum. Meeting this condition is required to ensure the stability of simulation. However, the condition (35) is not sufficient in the case of FDTD in the media described by the TF constitutive relations.

Following the standard derivation of the IO FDTD stability condition [9], the time-step limit is derived for FDTD in the media described by the TF constitutive relations based on (25)–(30)

$$\Delta t\le 2^{1-\frac{1}{\alpha}}\left(\frac{\sqrt{\mu_{\alpha}\varepsilon_{\alpha}}}{\sqrt{\frac{1}{(\Delta x)^2}+\frac{1}{(\Delta y)^2}+\frac{1}{(\Delta z)^2}}}\right)^{\frac{1}{\alpha}}. \tag{36}$$

The detailed derivation of (36) is presented in Appendices A–C. This new time-step limit is obtained through analysis of the numerical-dispersion relation. When $\alpha=1$ is assumed, the condition (36) simplifies to the IO case (35). In the considered one-dimensional simulation, the stability condition simplifies to

$$\Delta t\le 2^{1-\frac{1}{\alpha}}\left(\sqrt{\varepsilon_{\alpha}\mu_{\alpha}}\Delta z\right)^{\frac{1}{\alpha}}. \tag{37}$$

Let us verify numerically the condition (37). For this purpose, let us consider the simulation with an initial condition $E_x^0(k_s)=1$, while the field values at other spatial and temporal localizations are equal to zero. For a varying parameter $\frac{1}{2}<\alpha<1$, values of Δt around the analytical stability limit are considered. For each value of the time-step size, a short simulation is performed. In the case of the considered FO model, a decay in field amplitude is expected, which is further discussed in Section 5. Therefore, if the maximum value of the electric field at the end of the simulation is larger than one, it is considered as unstable. The results of numerical verification are presented in Figure 1, where the minimal unstable value of Δt is plotted along with the analytically obtained stability limit.

For each considered value of α, all the verified values of the time-step size below the limit (37) resulted in stable simulations, while all the values above this limit resulted in unstable ones. This confirms the correctness of the derived stability condition.

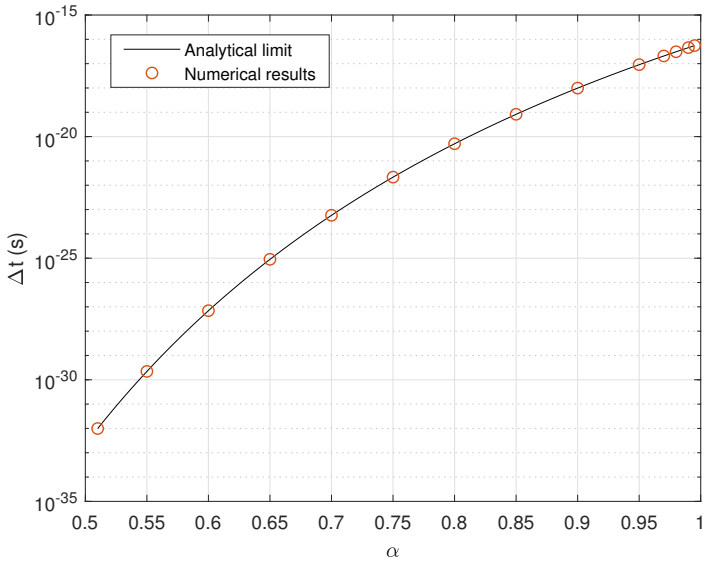

Figure 1. Stability limit for varying parameter α ($\Delta z = 0.02\,\mu$m).

5. Simulation Results

In this section, simulation results are presented for the FDTD method in the media described by the TF constitutive relations. For all the cases, unless stated otherwise, $\Delta z = 0.01\,\mu$m and the Courant coefficient is equal to 0.999, which means that Δt is equal to 0.999 of the stability limit given by (37). We focus on one-dimensional simulations due to the large computational overhead of the method, which includes the whole history of the electromagnetic field in the computations, as well as due to easy comparison with the results generated by the method presented in the literature.

5.1. Simulations of Wave Propagation

One-dimensional simulations of wave propagation are considered in a homogeneous FO medium, with the values of α slightly below the unit value. The source signal, in the form of a Gaussian-modulated sinusoidal pulse (presented in Figure 2), is injected 0.1 µm from the left boundary of the computational domain and propagates rightwards.

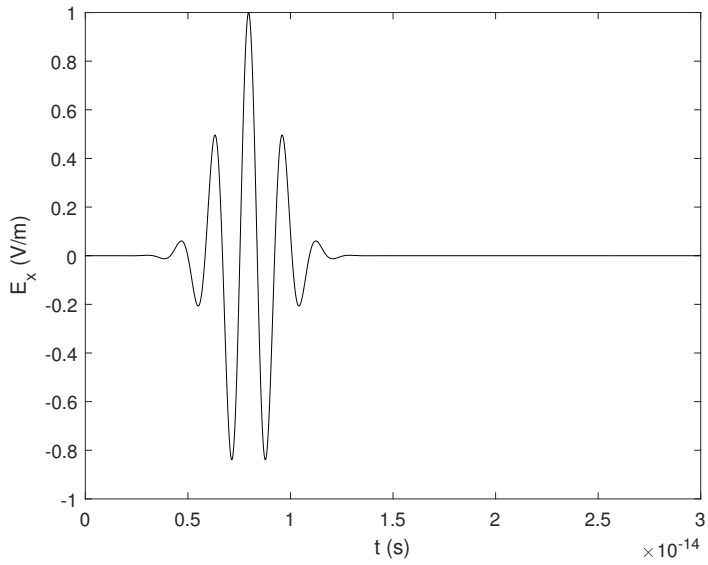

Figure 2. Source-signal waveform.

Results of the FDTD simulations in the form of the electric-field waveforms measured at the distance 10 µm from the source are presented in Figure 3.

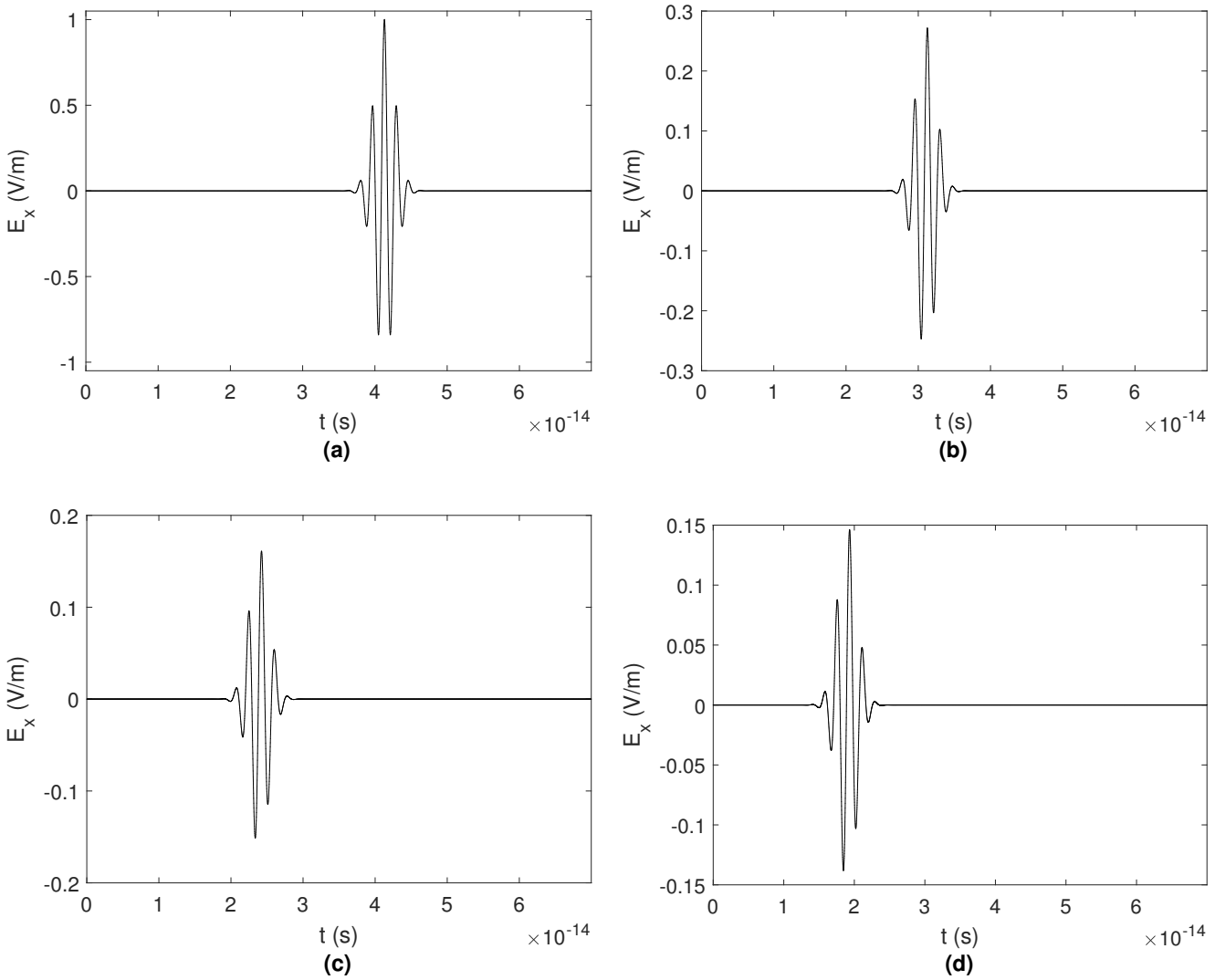

Figure 3. Electric-field waveforms measured 10 µm from source. (**a**) $\alpha = 1$. (**b**) $\alpha = 0.99$. (**c**) $\alpha = 0.98$. (**d**) $\alpha = 0.97$.

In the simulation with $\alpha = 1$, the pulse propagates without deformation. It is expected, because this case is equivalent to wave propagation in a vacuum. In other cases, wave attenuation and distortion are observed, which is consistent with the results in [22]. Furthermore, the pulse maximum is also observed earlier than in a vacuum. All the described effects (i.e., wave attenuation, dispersion, and increased group velocity) increase with the decrease in the parameter α.

The obtained results are compared with the results of the frequency-domain method presented in [22]. The electric-field waveforms are shown for different measurement positions in Figure 4. There are visible differences in the field values between the results of both methods, which diminish when the spatial-step size Δz is decreased for FO FDTD.

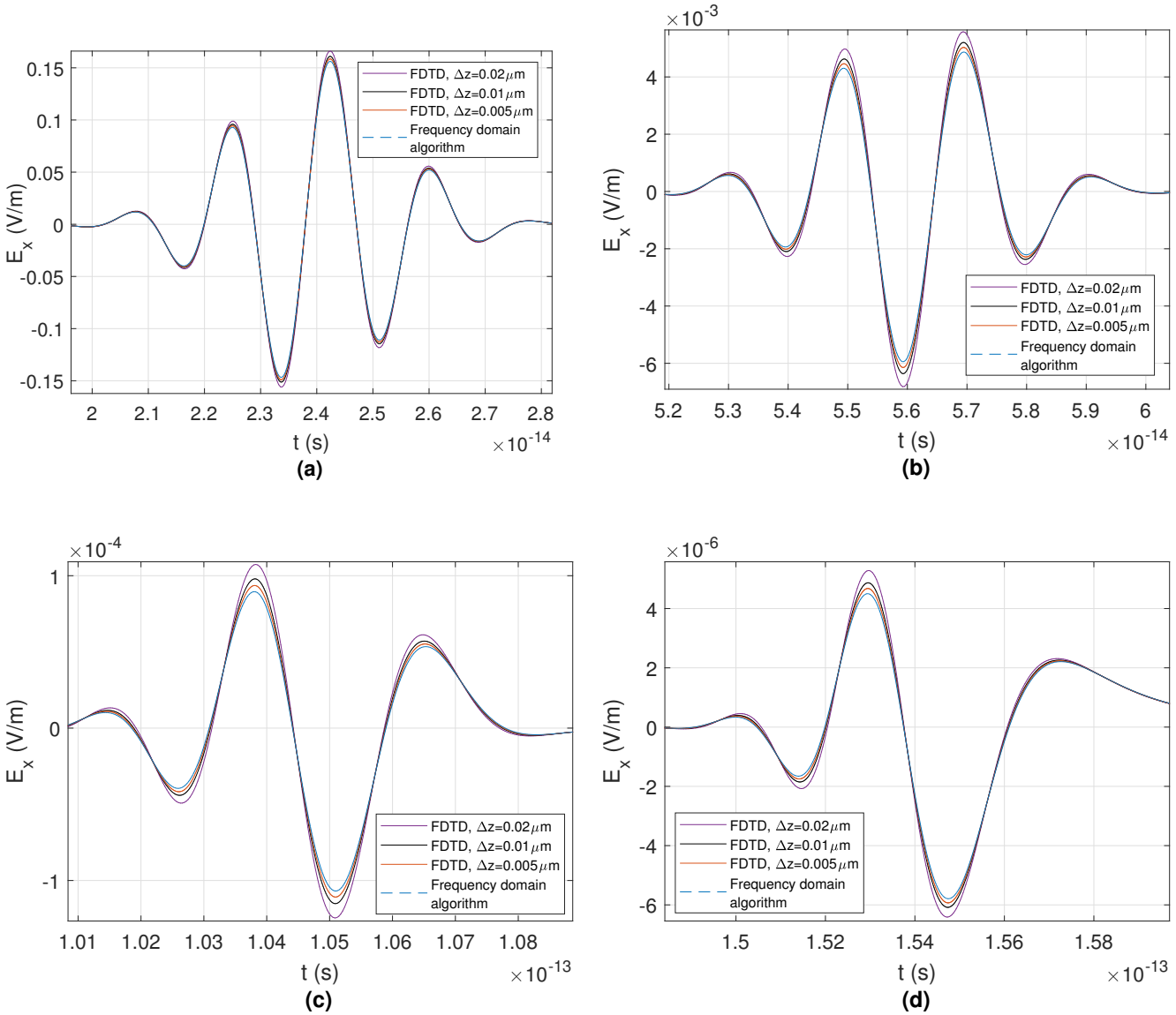

Figure 4. Comparison between results of FDTD with varying spatial-step size and frequency-domain simulations ($\alpha = 0.98$). Distance from source: (**a**) 10 µm. (**b**) 30 µm. (**c**) 60 µm. (**d**) 90 µm.

The differences between the waveforms are visible when the spatial resolution is insufficient in FO FDTD. It is clear, however, that the results of the FO FDTD simulations converge to those obtained using the frequency-domain method when the spatial-step size Δz is decreased. This confirms that the FO FDTD simulation method is developed correctly.

5.2. Simulations of Reflections

The FDTD method allows one to combine different materials in a single computational domain. Therefore, we consider a simulation of the wave propagating through a vacuum and impinging on a material described by the TF constitutive relations, with the parameter $\alpha = 0.99$. The results, in the form of electric-field distributions in the space for varying time, are presented in Figure 5.

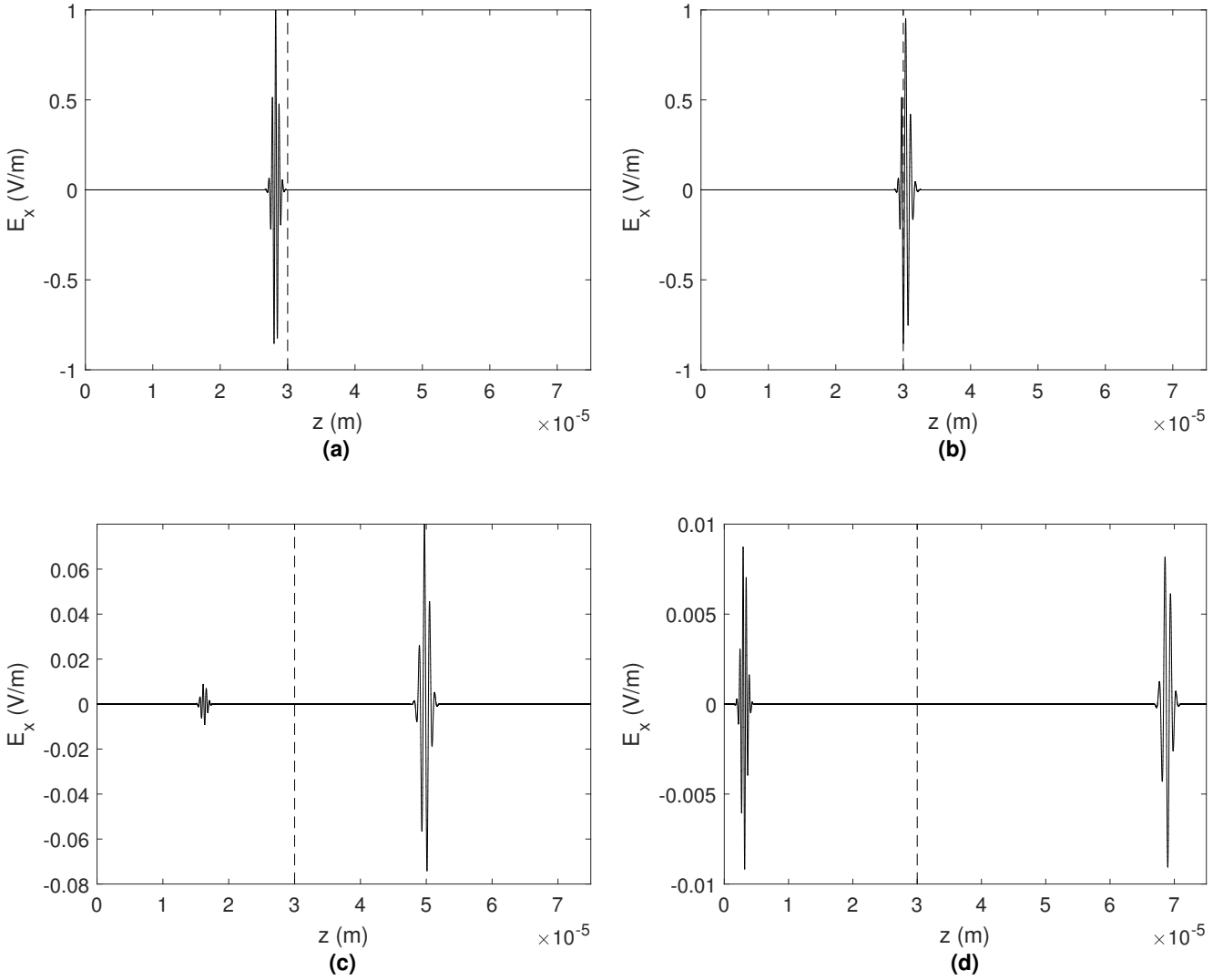

Figure 5. Spatial electric-field distribution for computational domain combining vacuum and FO material. Dashed line indicates boundary between materials, with vacuum on the left and FO material on the right side of line. Simulation results for time t: (**a**) 6.880×10^{-14} s. (**b**) 7.556×10^{-14} s. (**c**) 1.207×10^{-14} s. (**d**) 1.647×10^{-14} s.

The incident wave is almost completely transmitted into the FO material, with only a small reflection, as can be seen in Figure 5b,c. The ratio of the amplitude of the reflected wave to the amplitude of the incident wave is equal to 0.0091. The transmitted pulse is further attenuated while propagating through the FO medium. The incident Gaussian-modulated sinusoidal pulse is, however, also slightly distorted before arriving upon the boundary, as can be seen in Figure 5a. This is undesired behavior, as the wave should not experience any significant deformation or attenuation while travelling through a vacuum. This purely numerical distortion is a result of the Courant coefficient for a vacuum being significantly lower than 1, i.e., Δt is different than the magic time-step size, which provides accurate simulations in one-dimensional IO FDTD [9]. Such a value of the Courant coefficient is, however, necessary in order to ensure the stability of simulation in the FO medium.

6. Computational Complexity

Computational complexity is an important factor in numerical simulations. The IO FDTD algorithm has $O(n)$ complexity with regard to the number of iterations (i.e., time-

steps). In the case of FO FDTD, complexity increases to $O(n^2)$ because, in every iteration, all the previous electromagnetic-field values are included in the update procedure. The quadratic dependence on the number of time-steps is confirmed numerically, with the results presented in Figure 6. All the presented execution times are obtained with the use of an Intel(R) Core(TM) i7-8750H processor. The OpenMP-based parallelization is used in our code in order to distribute computations among the CPU cores.

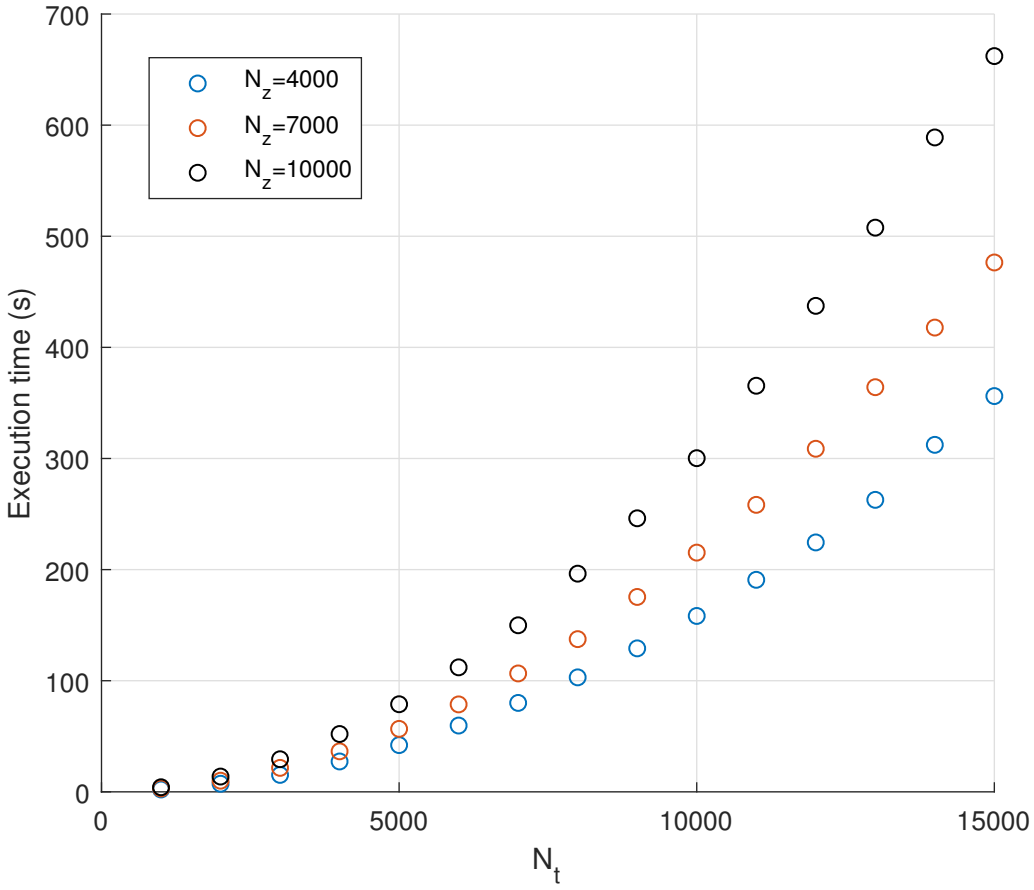

Figure 6. Dependence of execution time on iteration number N_t for $\alpha = 0.98$ and varying domain size N_z.

The execution time, depending on the size of the computational domain, is presented in Figure 7. The complexity is linear, i.e., the same as in the case of IO FDTD.

Apart from a larger time complexity, FO FDTD also suffers from a significantly larger memory demand. As all the previous field values need to be stored, the occupied memory grows linearly with time. In the IO case, on the other hand, it remains constant.

Higher computational and memory demands are further increased by the necessity of taking lower values of the time-step size in order to satisfy the stability condition (37). As can be seen in Figure 1, the stable Δt values are significantly lower than in the IO FDTD case, even for α near 1.

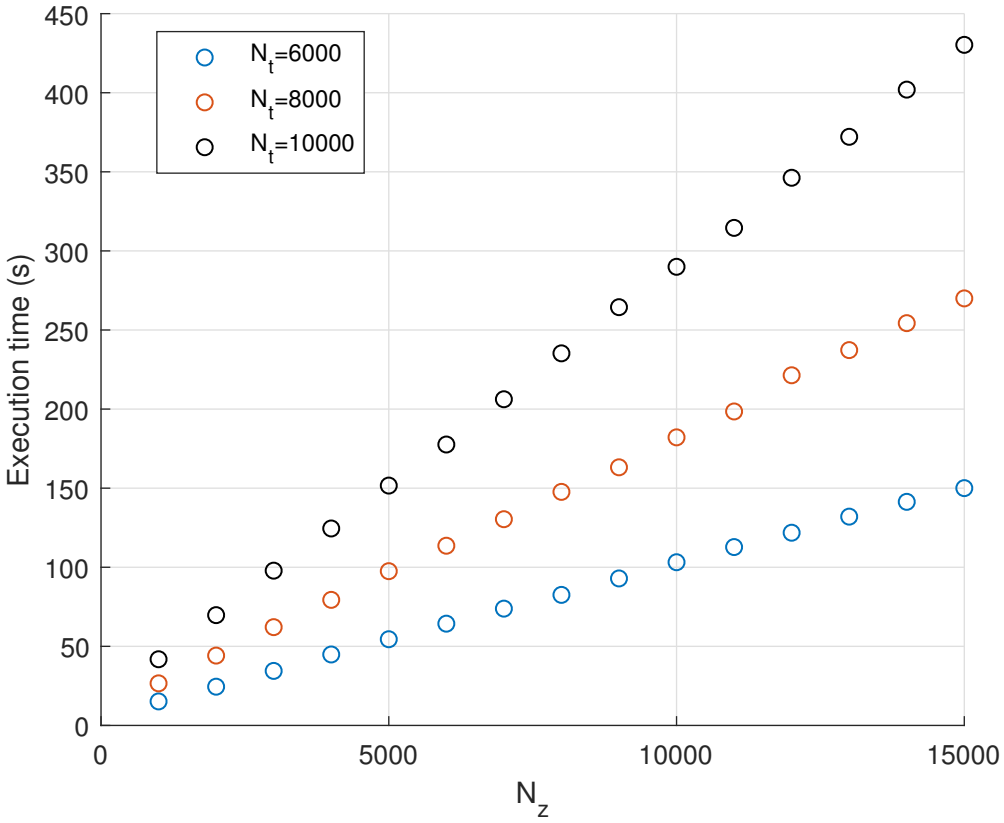

Figure 7. Dependence of execution time on domain size N_z for $\alpha = 0.98$ and varying iteration number N_t.

7. Conclusions

In this paper, the FDTD simulation method for wave propagation in the media described by the TF constitutive relations is presented. TF Maxwell's equations are derived based on these constitutive relations and the Grünwald–Letnikov definition of a fractional derivative. Then the FDTD algorithm, which includes memory effects and energy dissipation of the considered media, is introduced. The stability limit of the time-step size is derived for the proposed FDTD method which, to the best of our knowledge, has not been presented in the literature before. The obtained FDTD results are compared with those obtained with the use of the reference frequency-domain method already presented in the literature, and the compatibility between both methods is hereby demonstrated. Therefore, FDTD is proved to be an appropriate method for simulation of the FO media as well. High spatial resolution is required, however, to obtain accurate results. FO FDTD is, unfortunately, computation and memory demanding compared to the ordinary (i.e., IO) FDTD algorithm and, therefore, requires larger computational resources than in the IO case.

Our future research focus will include investigation of implicit FDTD schemes applied to the FO media, as well as consideration of their acceleration techniques.

Author Contributions: Conceptualization, P.P. and T.P.S.; methodology, P.P., T.P.S. and J.G.; validation, P.P. and J.G.; writing—original draft preparation, P.P., T.P.S. and J.G.; writing—review and editing, P.P., T.P.S. and J.G. All authors have read and agreed to the published version of the manuscript.

Funding: This research received no external funding.

Institutional Review Board Statement: Not applicable.

Informed Consent Statement: Not applicable.

Data Availability Statement: Not applicable.

Conflicts of Interest: The authors declare no conflict of interest.

Abbreviations

The following abbreviations are used in this manuscript:

FDTD	Finite-difference time-domain
TF	Time fractional
FO	Fractional order
IO	Integer order
ADE	Auxiliary differential equation

Appendix A. Derivation of Numerical-Dispersion Relation for FO FDTD

For clarity of presentation, the one-dimensional dispersion relation and stability condition are derived first, with subsequent generalisations to the three-dimensional case in Appendix C.

Let us consider one-dimensional discretized FO Maxwell's equations

$$\frac{E_x^n(k+1)-E_x^n(k)}{\Delta z}=-\mu_\alpha\left(\frac{1}{\Delta t}\right)^\alpha\sum_{l=0}^{n}w_l^\alpha H_y^{n-l+\frac{1}{2}}(k+\frac{1}{2}) \tag{A1}$$

$$-\frac{H_y^{n+\frac{1}{2}}(k+\frac{1}{2})-H_y^{n+\frac{1}{2}}(k-\frac{1}{2})}{\Delta z}=\varepsilon_\alpha\left(\frac{1}{\Delta t}\right)^\alpha\sum_{l=0}^{n}w_l^\alpha E_x^{n-l+1}(k). \tag{A2}$$

Let us assume the existence of harmonic solutions with the field distributions

$$\begin{aligned}H_y^n(k)&=H_{y0}e^{j(\tilde{\omega}n\Delta t-\tilde{k}_zk\Delta z)}\\E_x^n(k)&=E_{x0}e^{j(\tilde{\omega}n\Delta t-\tilde{k}_zk\Delta z)}\end{aligned} \tag{A3}$$

where $\tilde{\omega}\in\mathbb{C}$, $\tilde{k}_z\in\mathbb{R}$. Substituting (A3) into (A1) gives

$$H_{y0}\frac{\sum_{l=0}^{N}[w_l^\alpha e^{j\tilde{\omega}(n-l+\frac{1}{2})\Delta t}e^{-j\tilde{k}_z(k+\frac{1}{2})\Delta z}]}{(\Delta t)^\alpha}=-\frac{1}{\mu_\alpha}E_{x0}\frac{e^{j\tilde{\omega}n\Delta t}e^{-j\tilde{k}_z(k+1)\Delta z}-e^{j\tilde{\omega}n\Delta t}e^{-j\tilde{k}_zk\Delta z}}{\Delta z} \tag{A4}$$

$$\begin{aligned}H_{y0}&=-\frac{(\Delta t)^\alpha E_{x0}}{\mu_\alpha\Delta z}\frac{e^{j\tilde{\omega}n\Delta t}e^{-j\tilde{k}_z(k+\frac{1}{2})\Delta z}\left(e^{-j\tilde{k}_z(\frac{1}{2})\Delta z}-e^{-j\tilde{k}_z(-\frac{1}{2})\Delta z}\right)}{e^{-j\tilde{k}_z(k+\frac{1}{2})\Delta z}\sum_{l=0}^{N}w_l^\alpha e^{j\tilde{\omega}(n-l+\frac{1}{2})\Delta t}}\\&=\frac{(\Delta t)^\alpha E_{x0}}{\mu_\alpha\Delta z}\frac{e^{j\tilde{\omega}n\Delta t}\left(e^{j\tilde{k}_z\frac{1}{2}\Delta z}-e^{-j\tilde{k}_z\frac{1}{2}\Delta z}\right)}{e^{j\tilde{\omega}n\Delta t}\sum_{l=0}^{N}w_l^\alpha e^{j\tilde{\omega}(-l+\frac{1}{2})\Delta t}}\\&=\frac{(\Delta t)^\alpha E_{x0}}{\mu_\alpha\Delta z}\frac{2j\frac{e^{j\tilde{k}_z\frac{1}{2}\Delta z}-e^{-j\tilde{k}_z\frac{1}{2}\Delta z}}{2j}}{\sum_{l=0}^{N}w_l^\alpha e^{j\tilde{\omega}(-l+\frac{1}{2})\Delta t}}\\&=E_{x0}\frac{(\Delta t)^\alpha}{\mu_\alpha\Delta z}\frac{2j\sin\left(\frac{\tilde{k}_z\Delta z}{2}\right)}{\sum_{l=0}^{N}w_l^\alpha e^{j\tilde{\omega}(-l+\frac{1}{2})\Delta t}}.\end{aligned} \tag{A5}$$

After substituting (A3) into (A2), one obtains

$$E_{x0}\frac{\sum_{l=0}^{N}[w_l^\alpha e^{j\tilde{\omega}(n-l+1)\Delta t}e^{-j\tilde{k}_zk\Delta z}]}{(\Delta t)^\alpha}=-\frac{1}{\varepsilon_\alpha}H_{y0}\frac{e^{j\tilde{\omega}(n+\frac{1}{2})\Delta t}e^{-j\tilde{k}_z(k+\frac{1}{2})\Delta z}-e^{j\tilde{\omega}(n+\frac{1}{2})\Delta t}e^{-j\tilde{k}_z(k-\frac{1}{2})\Delta z}}{\Delta z} \tag{A6}$$

$$\begin{aligned} E_{x0} &= -\frac{(\Delta t)^{\alpha} H_{y0}}{\varepsilon_{\alpha} \Delta z} \frac{e^{j\tilde{\omega}(n+\frac{1}{2})\Delta t} e^{-j\tilde{k}_z k\Delta z} \left(e^{-j\tilde{k}_z \frac{1}{2}\Delta z} - e^{-j\tilde{k}_z(-\frac{1}{2})\Delta z} \right)}{e^{-j\tilde{k}_z k\Delta z} \sum_{l=0}^{N} w_l^{\alpha} e^{j\tilde{\omega}(n-l+1)\Delta t}} \\ &= \frac{(\Delta t)^{\alpha} H_{y0}}{\varepsilon_{\alpha} \Delta z} \frac{e^{j\tilde{\omega}(n+\frac{1}{2})\Delta t} \left(e^{j\tilde{k}_z \frac{1}{2}\Delta z} - e^{-j\tilde{k}_z \frac{1}{2}\Delta z} \right)}{e^{j\tilde{\omega}(n+\frac{1}{2})\Delta t} \sum_{l=0}^{N} w_l^{\alpha} e^{j\tilde{\omega}(-l+\frac{1}{2})\Delta t}} \\ &= \frac{(\Delta t)^{\alpha} H_{y0}}{\varepsilon_{\alpha} \Delta z} \frac{2j \frac{e^{j\tilde{k}_z \frac{1}{2}\Delta z} - e^{-j\tilde{k}_z \frac{1}{2}\Delta z}}{2j}}{\sum_{l=0}^{N} w_l^{\alpha} e^{j\tilde{\omega}(-l+\frac{1}{2})\Delta t}} \\ &= H_{y0} \frac{(\Delta t)^{\alpha}}{\varepsilon_{\alpha} \Delta z} \frac{2j \sin\left(\frac{\tilde{k}_z \Delta z}{2} \right)}{\sum_{l=0}^{N} w_l^{\alpha} e^{j\tilde{\omega}(-l+\frac{1}{2})\Delta t}}. \end{aligned} \tag{A7}$$

Further, substituting the result of (A5) for H_{y0} into (A7) gives

$$E_{x0} = E_{x0} \frac{(\Delta t)^{\alpha}}{\mu_{\alpha} \Delta z} \frac{2j \sin\left(\frac{\tilde{k}_z \Delta z}{2} \right)}{\sum_{l=0}^{N} w_l^{\alpha} e^{j\tilde{\omega}(-l+\frac{1}{2})\Delta t}} \frac{(\Delta t)^{\alpha}}{\varepsilon_{\alpha} \Delta z} \frac{2j \sin\left(\frac{\tilde{k}_z \Delta z}{2} \right)}{\sum_{l=0}^{N} w_l^{\alpha} e^{j\tilde{\omega}(-l+\frac{1}{2})\Delta t}} \tag{A8}$$

$$\left(\frac{\sum_{l=0}^{N} w_l^{\alpha} e^{j\tilde{\omega}(-l+\frac{1}{2})\Delta t}}{2j} \right)^2 = \frac{(\Delta t)^{2\alpha}}{\varepsilon_{\alpha} \mu_{\alpha} (\Delta z)^2} \left[\sin\left(\frac{\tilde{k}_z \Delta z}{2} \right) \right]^2. \tag{A9}$$

The coefficients of the Grünwald–Letnikov derivative w_l^{α} satisfy the condition [27]

$$\sum_{l=0}^{\infty} w_l^{\alpha} z^l = (1 - z)^{\alpha} \tag{A10}$$

where $z \in \mathbb{C}$. Let us transform the left-hand side of (A9) into

$$\begin{aligned} \left(\frac{\sum_{l=0}^{N} w_l^{\alpha} e^{j\tilde{\omega}(-l+\frac{1}{2})\Delta t}}{2j} \right)^2 &= \left(\frac{e^{j\tilde{\omega}\frac{1}{2}\Delta t} \sum_{l=0}^{N} w_l^{\alpha} e^{j\tilde{\omega}(-l)\Delta t}}{2j} \right)^2 \\ &= \left(\frac{e^{j\tilde{\omega}\frac{1}{2}\Delta t} \sum_{l=0}^{N} w_l^{\alpha} (e^{-j\tilde{\omega}\Delta t})^l}{2j} \right)^2 \quad \text{(using (A10))} \\ &\approx \left(\frac{e^{j\tilde{\omega}\Delta t\frac{1}{2}} \left(1 - e^{-j\tilde{\omega}\Delta t}\right)^{\alpha}}{2j} \right)^2. \end{aligned} \tag{A11}$$

As a result, one obtains the numerical-dispersion relation for the FO FDTD algorithm

$$\left(\frac{e^{j\tilde{\omega}\Delta t\frac{1}{2}} \left(1 - e^{-j\tilde{\omega}\Delta t}\right)^{\alpha}}{2j} \right)^2 = \frac{(\Delta t)^{2\alpha}}{\varepsilon_{\alpha} \mu_{\alpha} (\Delta z)^2} \left[\sin\left(\frac{\tilde{k}_z \Delta z}{2} \right) \right]^2. \tag{A12}$$

This equation is an equivalent of the IO FDTD numerical-dispersion relation, i.e., the Formula (4.12) in [9].

Appendix B. Derivation of Stability Condition for FO FDTD

Further transformation of (A12) gives

$$e^{j\tilde{\omega}\Delta t\frac{1}{2\alpha}} \left(1 - e^{-j\tilde{\omega}\Delta t}\right) = (2j)^{\frac{1}{\alpha}} \underbrace{\frac{\Delta t}{\left(\sqrt{\varepsilon_{\alpha}\mu_{\alpha}}\Delta z\right)^{\frac{1}{\alpha}}} \left| \sin\left(\frac{\tilde{k}_z \Delta z}{2} \right) \right|^{\frac{1}{\alpha}}}_{=\tilde{\zeta}_{\alpha}}. \tag{A13}$$

After substituting $\tilde{\omega} = \tilde{\omega}_r + j\tilde{\omega}_i$, one obtains

$$e^{\frac{-\tilde{\omega}_i \Delta t}{2\alpha}} e^{j\frac{\tilde{\omega}_r \Delta t}{2\alpha}} \left(1 - e^{\tilde{\omega}_i \Delta t} e^{-j\tilde{\omega}_r \Delta t}\right) = (2j)^{\frac{1}{\alpha}} \xi_\alpha. \tag{A14}$$

Then, $1 - e^{\tilde{\omega}_i \Delta t} e^{-j\tilde{\omega}_r \Delta t}$ can be expressed in the exponential form as follows:

$$\begin{aligned} 1 - e^{\tilde{\omega}_i \Delta t} e^{-j\tilde{\omega}_r \Delta t} &= 1 - e^{\tilde{\omega}_i \Delta t}[\cos(-\tilde{\omega}_r \Delta t) + j\sin(-\tilde{\omega}_r \Delta t)] \\ &= 1 - e^{\tilde{\omega}_i \Delta t}\cos(\tilde{\omega}_r \Delta t) + j e^{\tilde{\omega}_i \Delta t}\sin(\tilde{\omega}_r \Delta t) \\ &= \sqrt{[1 - e^{\tilde{\omega}_i \Delta t}\cos(\tilde{\omega}_r \Delta t)]^2 + [e^{\tilde{\omega}_i \Delta t}\sin(\tilde{\omega}_r \Delta t)]^2}\, e^{j\,\mathrm{arctg2}\left[e^{\tilde{\omega}_i \Delta t}\sin(\tilde{\omega}_r \Delta t), 1 - e^{\tilde{\omega}_i \Delta t}\cos(\tilde{\omega}_r \Delta t)\right]}. \end{aligned} \tag{A15}$$

Hence, one obtains

$$\begin{aligned} \left|1 - e^{\tilde{\omega}_i \Delta t} e^{-j\tilde{\omega}_r \Delta t}\right| &= \sqrt{[1 - e^{\tilde{\omega}_i \Delta t}\cos(\tilde{\omega}_r \Delta t)]^2 + [e^{\tilde{\omega}_i \Delta t}\sin(\tilde{\omega}_r \Delta t)]^2} \\ &= \sqrt{1 - 2e^{\tilde{\omega}_i \Delta t}\cos(\tilde{\omega}_r \Delta t) + e^{2\tilde{\omega}_i \Delta t}\cos^2(\tilde{\omega}_r \Delta t) + e^{2\tilde{\omega}_i \Delta t}\sin^2(\tilde{\omega}_r \Delta t)} \\ &= \sqrt{1 - 2e^{\tilde{\omega}_i \Delta t}\cos(\tilde{\omega}_r \Delta t) + e^{2\tilde{\omega}_i \Delta t}} \end{aligned} \tag{A16}$$

$$\mathrm{Arg}\left(1 - e^{\tilde{\omega}_i \Delta t} e^{-j\tilde{\omega}_r \Delta t}\right) = \mathrm{arctg2}\left[e^{\tilde{\omega}_i \Delta t}\sin(\tilde{\omega}_r \Delta t), 1 - e^{\tilde{\omega}_i \Delta t}\cos(\tilde{\omega}_r \Delta t)\right]. \tag{A17}$$

Finally, one obtains

$$\left|e^{\frac{-\tilde{\omega}_i \Delta t}{2\alpha}} e^{j\frac{\tilde{\omega}_r \Delta t}{2\alpha}} \left(1 - e^{\tilde{\omega}_i \Delta t} e^{-j\tilde{\omega}_r \Delta t}\right)\right| = e^{-\frac{\tilde{\omega}_i \Delta t}{2\alpha}} \sqrt{1 - 2e^{\tilde{\omega}_i \Delta t}\cos(\tilde{\omega}_r \Delta t) + e^{2\tilde{\omega}_i \Delta t}} \tag{A18}$$

$$\mathrm{Arg}\left(e^{\frac{-\tilde{\omega}_i \Delta t}{2\alpha}} e^{j\frac{\tilde{\omega}_r \Delta t}{2\alpha}} \left[1 - e^{\tilde{\omega}_i \Delta t} e^{-j\tilde{\omega}_r \Delta t}\right]\right) = \frac{\tilde{\omega}_r \Delta t}{2\alpha} + \mathrm{arctg2}\left[e^{\tilde{\omega}_i \Delta t}\sin(\tilde{\omega}_r \Delta t), 1 - e^{\tilde{\omega}_i \Delta t}\cos(\tilde{\omega}_r \Delta t)\right]. \tag{A19}$$

Comparing modules and arguments of the left- and right-hand sides of (A14), one obtains

$$e^{-\frac{\tilde{\omega}_i \Delta t}{2\alpha}} \sqrt{1 - 2e^{\tilde{\omega}_i \Delta t}\cos(\tilde{\omega}_r \Delta t) + e^{2\tilde{\omega}_i \Delta t}} = 2^{\frac{1}{\alpha}} \xi_\alpha \tag{A20}$$

$$\frac{\tilde{\omega}_r \Delta t}{2\alpha} + \mathrm{arctg2}\left[e^{\tilde{\omega}_i \Delta t}\sin(\tilde{\omega}_r \Delta t), 1 - e^{\tilde{\omega}_i \Delta t}\cos(\tilde{\omega}_r \Delta t)\right] = \frac{\pi}{2\alpha}. \tag{A21}$$

Analyzing the argument relation (A21), one obtains

$$\frac{e^{\tilde{\omega}_i \Delta t}\sin(\tilde{\omega}_r \Delta t)}{1 - e^{\tilde{\omega}_i \Delta t}\cos(\tilde{\omega}_r \Delta t)} = \mathrm{tg}\left(\frac{\pi - \tilde{\omega}_r \Delta t}{2\alpha}\right). \tag{A22}$$

The sampling time Δt must respect the Nyquist theorem; therefore, the only proper solution to (A22) is $\tilde{\omega}_r = \frac{\pi}{\Delta t}$. Let us substitute $\cos(\tilde{\omega}_r \Delta t) = \cos\left(\frac{\pi}{\Delta t}\Delta t\right) = \cos(\pi) = -1$ into the left-hand side of (A20), which gives

$$\begin{aligned} e^{-\frac{\tilde{\omega}_i \Delta t}{2\alpha}} \sqrt{1 + 2e^{\tilde{\omega}_i \Delta t} + e^{2\tilde{\omega}_i \Delta t}} &= e^{-\frac{\tilde{\omega}_i \Delta t}{2\alpha}} \sqrt{(e^{\tilde{\omega}_i \Delta t} + 1)^2} \\ &= e^{-\frac{\tilde{\omega}_i \Delta t}{2\alpha}} (e^{\tilde{\omega}_i \Delta t} + 1). \end{aligned} \tag{A23}$$

Let us introduce auxiliary variables $e^{\tilde{\omega}_i \Delta t} = u$ and $\frac{1}{2\alpha} = \beta$. Using (A20) and (A23), one then obtains

$$u^{-\beta}(1 + u) = 2^{\frac{1}{\alpha}} \xi_\alpha \tag{A24}$$

where $\frac{1}{2} < \alpha < 1$, $\frac{1}{2} < \beta < 1$. Equation (A24) can be written as

$$u + 1 = 2^{\frac{1}{\alpha}} \xi_\alpha u^\beta. \tag{A25}$$

A simulation is stable when $\tilde{\omega}_i \geq 0$, which is equivalent to $u = e^{\tilde{\omega}_i \Delta t} \geq 1$. Equation (A25) is solved graphically and visualised in Figure A1. For ξ_α larger than the boundary value equal 2, (A25) has two solutions, i.e., one smaller and one larger than 1. In this case a simulation is considered unstable. A smaller value of ξ_α means that either two solutions larger than 1, one such solution, or even no such solutions exist. All these cases are considered to be stable, as they lack any unstable term smaller than 1.

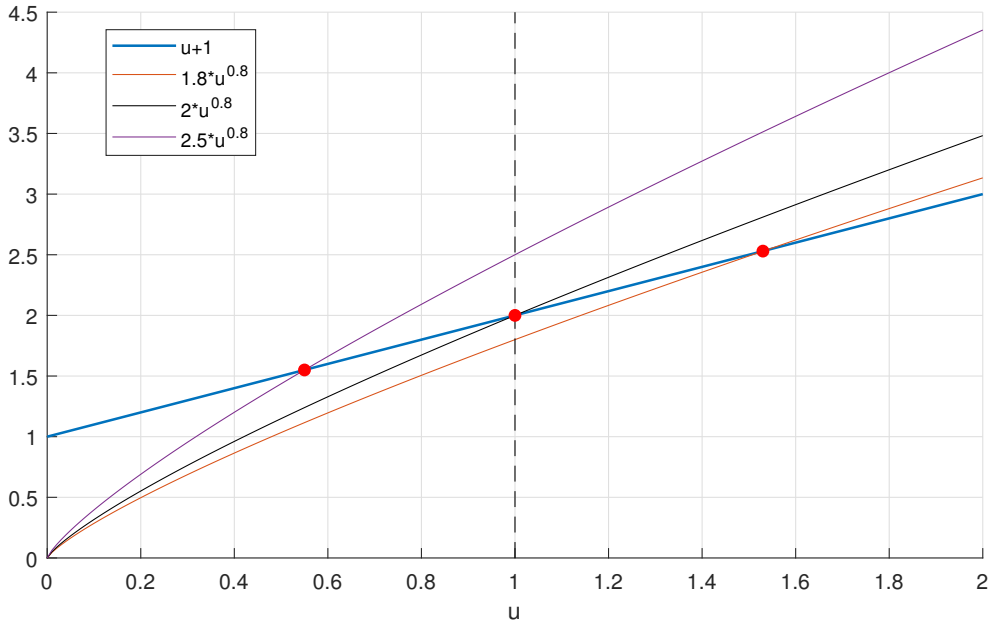

Figure A1. Points of intersection of functions $u + 1$ and $2^{\frac{1}{\alpha}} \xi_\alpha u^\beta$ for different values of $2^{\frac{1}{\alpha}} \xi_\alpha$.

Hence, the stability condition can be written as

$$2^{\frac{1}{\alpha}} \xi_\alpha \leq 2. \tag{A26}$$

After expanding ξ_α, (A26) gives

$$2^{\frac{1}{\alpha}} \frac{\Delta t}{(\sqrt{\varepsilon_\alpha \mu_\alpha} \Delta z)^{\frac{1}{\alpha}}} \left| \sin\left(\frac{\tilde{k}_z \Delta z}{2} \right) \right|^{\frac{1}{\alpha}} \leq 2. \tag{A27}$$

Transforming further, one obtains

$$\Delta t \leq 2^{1-\frac{1}{\alpha}} (\sqrt{\varepsilon_\alpha \mu_\alpha} \Delta z)^{\frac{1}{\alpha}} \frac{1}{\left| \sin\left(\frac{\tilde{k}_z \Delta z}{2} \right) \right|^{\frac{1}{\alpha}}}. \tag{A28}$$

The minimum value of $\frac{1}{\left| \sin\left(\frac{\tilde{k}_z \Delta z}{2} \right) \right|^{\frac{1}{\alpha}}}$ is equal to 1. The stability condition can therefore be written in its final form

$$\Delta t \leq 2^{1-\frac{1}{\alpha}} (\sqrt{\varepsilon_\alpha \mu_\alpha} \Delta z)^{\frac{1}{\alpha}}. \tag{A29}$$

Taking $\alpha = 1$, one obtains the standard Courant condition for one-dimensional IO FDTD

$$\Delta t \leq \sqrt{\varepsilon_0 \mu_0} \Delta z. \tag{A30}$$

Appendix C. Generalization of Stability Condition Towards Three-Dimensional FO FDTD

In the case of three-dimensional FO FDTD, discrete Maxwell's equations are considered

$$\left(\frac{1}{\Delta t}\right)^{\alpha}\sum_{l=0}^{n} w_l^{\alpha} H_x^{n-l+\frac{1}{2}}(I, J+\frac{1}{2}, K+\frac{1}{2}) = \frac{1}{\mu_\alpha}\left(\frac{E_y^n(I, J+\frac{1}{2}, K+1) - E_y^n(I, J+\frac{1}{2}, K)}{\Delta z} - \frac{E_z^n(I, J+1, K+\frac{1}{2}) - E_z^n(I, J, K+\frac{1}{2})}{\Delta y}\right) \tag{A31}$$

$$\left(\frac{1}{\Delta t}\right)^{\alpha}\sum_{l=0}^{n} w_l^{\alpha} H_y^{n-l+\frac{1}{2}}(I+\frac{1}{2}, J, K+\frac{1}{2}) = \frac{1}{\mu_\alpha}\left(\frac{E_z^n(I+1, J, K+\frac{1}{2}) - E_z^n(I, J, K+\frac{1}{2})}{\Delta x} - \frac{E_x^n(I+\frac{1}{2}, J, K+1) - E_x^n(I+\frac{1}{2}, J, K)}{\Delta z}\right) \tag{A32}$$

$$\left(\frac{1}{\Delta t}\right)^{\alpha}\sum_{l=0}^{n} w_l^{\alpha} H_z^{n-l+\frac{1}{2}}(I+\frac{1}{2}, J+\frac{1}{2}, K) = \frac{1}{\mu_\alpha}\left(\frac{E_x^n(I+\frac{1}{2}, J+1, K) - E_x^n(I+\frac{1}{2}, J, K)}{\Delta y} - \frac{E_y^n(I+1, J+\frac{1}{2}, K) - E_y^n(I, J+\frac{1}{2}, K)}{\Delta x}\right) \tag{A33}$$

$$\left(\frac{1}{\Delta t}\right)^{\alpha}\sum_{l=0}^{n} w_l^{\alpha} E_x^{n-l+1}(I+\frac{1}{2}, J, K) = \frac{1}{\varepsilon_\alpha}\left(\frac{H_z^{n+\frac{1}{2}}(I+\frac{1}{2}, J+\frac{1}{2}, K) - H_z^{n+\frac{1}{2}}(I+\frac{1}{2}, J-\frac{1}{2}, K)}{\Delta y} - \frac{H_y^{n+\frac{1}{2}}(I+\frac{1}{2}, J, K+\frac{1}{2}) - H_y^{n+\frac{1}{2}}(I+\frac{1}{2}, J+\frac{1}{2}, K-\frac{1}{2})}{\Delta z}\right) \tag{A34}$$

$$\left(\frac{1}{\Delta t}\right)^{\alpha}\sum_{l=0}^{n} w_l^{\alpha} E_y^{n-l+1}(I, J+\frac{1}{2}, K) = \frac{1}{\varepsilon_\alpha}\left(\frac{H_x^{n+\frac{1}{2}}(I, J+\frac{1}{2}, K+\frac{1}{2}) - H_x^{n+\frac{1}{2}}(I, J+\frac{1}{2}, K-\frac{1}{2})}{\Delta z} - \frac{H_z^{n+\frac{1}{2}}(I+\frac{1}{2}, J+\frac{1}{2}, K) - H_z^{n+\frac{1}{2}}(I-\frac{1}{2}, J+\frac{1}{2}, K)}{\Delta x}\right) \tag{A35}$$

$$\left(\frac{1}{\Delta t}\right)^{\alpha}\sum_{l=0}^{n} w_l^{\alpha} E_z^{n-l+1}(I, J, K+\frac{1}{2}) = \frac{1}{\varepsilon_\alpha}\left(\frac{H_y^{n+\frac{1}{2}}(I+\frac{1}{2}, J, K+\frac{1}{2}) - H_y^{n+\frac{1}{2}}(I-\frac{1}{2}, J, K+\frac{1}{2})}{\Delta x} - \frac{H_x^{n+\frac{1}{2}}(I, J+\frac{1}{2}, K+\frac{1}{2}) - H_x^{n+\frac{1}{2}}(I, J-\frac{1}{2}, K+\frac{1}{2})}{\Delta y}\right) \tag{A36}$$

where I, J, K denote coordinate indices in respective directions. Capital letters are used to differentiate these parameters from the imaginary unit $j = \sqrt{-1}$. Similarly, as in the one-dimensional case, the following assumptions regarding harmonic solutions are taken

$$\begin{aligned}
H_x^n(I, J, K) &= H_{x0} e^{j(\tilde{\omega} n\Delta t - \tilde{i}_x I\Delta x - \tilde{j}_y J\Delta y - \tilde{k}_z K\Delta z)} \\
H_y^n(I, J, K) &= H_{y0} e^{j(\tilde{\omega} n\Delta t - \tilde{i}_x I\Delta x - \tilde{j}_y J\Delta y - \tilde{k}_z K\Delta z)} \\
H_z^n(I, J, K) &= H_{z0} e^{j(\tilde{\omega} n\Delta t - \tilde{i}_x I\Delta x - \tilde{j}_y J\Delta y - \tilde{k}_z K\Delta z)} \\
E_x^n(I, J, K) &= E_{x0} e^{j(\tilde{\omega} n\Delta t - \tilde{i}_x I\Delta x - \tilde{j}_y J\Delta y - \tilde{k}_z K\Delta z)} \\
E_y^n(I, J, K) &= E_{y0} e^{j(\tilde{\omega} n\Delta t - \tilde{i}_x I\Delta x - \tilde{j}_y J\Delta y - \tilde{k}_z K\Delta z)} \\
E_z^n(I, J, K) &= E_{z0} e^{j(\tilde{\omega} n\Delta t - \tilde{i}_x I\Delta x - \tilde{j}_y J\Delta y - \tilde{k}_z K\Delta z)}
\end{aligned} \tag{A37}$$

where $\tilde{\omega} \in \mathbb{C}$ and $[\tilde{i}_x, \tilde{j}_y, \tilde{k}_z]$ (where $\tilde{i}_x, \tilde{j}_y, \tilde{k}_z \in \mathbb{R}$) is the numerical wavevector. Substituting (A37) into (A31)–(A36) gives

$$\left(\frac{1}{\Delta t}\right)^{\alpha} H_{x0} = \frac{1}{\mu_\alpha z_s}\left(E_{y0}\frac{e^{-j[\tilde{i}_x I\Delta x+\tilde{j}_y(J+\frac{1}{2})\Delta y+\tilde{k}_z(K+1)\Delta z]} - e^{-j[\tilde{i}_x I\Delta x+\tilde{j}_y(J+\frac{1}{2})\Delta y+\tilde{k}_z K\Delta z]}}{e^{-j[\tilde{i}_x I\Delta x+\tilde{j}_y(J+\frac{1}{2})\Delta y+\tilde{k}_z(K+\frac{1}{2})\Delta z]}\Delta z} - E_{z0}\frac{e^{-j[\tilde{i}_x I\Delta x+\tilde{j}_y(J+1)\Delta y+\tilde{k}_z(K+\frac{1}{2})\Delta z]} - e^{-j[\tilde{i}_x I\Delta x+\tilde{j}_y J\Delta y+\tilde{k}_z(K+\frac{1}{2})\Delta z]}}{e^{-j[\tilde{i}_x I\Delta x+\tilde{j}_y(J+\frac{1}{2})\Delta y+\tilde{k}_z(K+\frac{1}{2})\Delta z]}\Delta y}\right) \tag{A38}$$

$$\left(\frac{1}{\Delta t}\right)^{\alpha} H_{y0} = \frac{1}{\mu_\alpha z_s}\left(E_{z0}\frac{e^{-j[\tilde{i}_x(I+1)\Delta x+\tilde{j}_y J\Delta y+\tilde{k}_z(K+\frac{1}{2})\Delta z]} - e^{-j[\tilde{i}_x I\Delta x+\tilde{j}_y J\Delta y+\tilde{k}_z(K+\frac{1}{2})\Delta z]}}{e^{-j[\tilde{i}_x(I+\frac{1}{2})\Delta x+\tilde{j}_y J\Delta y+\tilde{k}_z(K+\frac{1}{2})\Delta z]}\Delta x} - E_{x0}\frac{e^{-j[\tilde{i}_x(I+\frac{1}{2})\Delta x+\tilde{j}_y J\Delta y+\tilde{k}_z(K+1)\Delta z]} - e^{-j[\tilde{i}_x(I+\frac{1}{2})\Delta x+\tilde{j}_y J\Delta y+\tilde{k}_z K\Delta z]}}{e^{-j[\tilde{i}_x(I+\frac{1}{2})\Delta x+\tilde{j}_y J\Delta y+\tilde{k}_z(K+\frac{1}{2})\Delta z]}\Delta z}\right) \tag{A39}$$

$$\left(\frac{1}{\Delta t}\right)^{\alpha} H_{z0} = \frac{1}{\mu_\alpha z_s}\left(E_{x0}\frac{e^{-j[\tilde{i}_x(I+\frac{1}{2})\Delta x+\tilde{j}_y(J+1)\Delta y+\tilde{k}_z K\Delta z]} - e^{-j[\tilde{i}_x(I+\frac{1}{2})\Delta x+\tilde{j}_y J\Delta y+\tilde{k}_z K\Delta z]}}{e^{-j[\tilde{i}_x(I+\frac{1}{2})\Delta x+\tilde{j}_y(J+\frac{1}{2})\Delta y+\tilde{k}_z K\Delta z]}\Delta y} - E_{y0}\frac{e^{-j[\tilde{i}_x(I+1)\Delta x+\tilde{j}_y(J+\frac{1}{2})\Delta y+\tilde{k}_z K\Delta z]} - e^{-j[\tilde{i}_x I\Delta x+\tilde{j}_y(J+\frac{1}{2})\Delta y+\tilde{k}_z K\Delta z]}}{e^{-j[\tilde{i}_x(I+\frac{1}{2})\Delta x+\tilde{j}_y(J+\frac{1}{2})\Delta y+\tilde{k}_z K\Delta z]}\Delta x}\right) \tag{A40}$$

$$\left(\frac{1}{\Delta t}\right)^{\alpha} E_{x0} = \frac{1}{\varepsilon_\alpha z_s}\left(H_{z0}\frac{e^{-j[\tilde{i}_x(I+\frac{1}{2})\Delta x+\tilde{j}_y(J+\frac{1}{2})\Delta y+\tilde{k}_z K\Delta z]} - e^{-j[\tilde{i}_x(I+\frac{1}{2})\Delta x+\tilde{j}_y(J-\frac{1}{2})\Delta y+\tilde{k}_z K\Delta z]}}{e^{-j[\tilde{i}_x(I+\frac{1}{2})\Delta x+\tilde{j}_y J\Delta y+\tilde{k}_z K\Delta z]}\Delta y} - H_{y0}\frac{e^{-j[\tilde{i}_x(I+\frac{1}{2})\Delta x+\tilde{j}_y J\Delta y+\tilde{k}_z(K+\frac{1}{2})\Delta z]} - e^{-j[\tilde{i}_x(I+\frac{1}{2})\Delta x+\tilde{j}_y J\Delta y+\tilde{k}_z(K-\frac{1}{2})\Delta z]}}{e^{-j[\tilde{i}_x(I+\frac{1}{2})\Delta x+\tilde{j}_y J\Delta y+\tilde{k}_z K\Delta z]}\Delta z}\right) \tag{A41}$$

$$\left(\frac{1}{\Delta t}\right)^{\alpha} E_{y0} = \frac{1}{\varepsilon_\alpha z_s}\left(H_{x0}\frac{e^{-j[\tilde{i}_x I\Delta x+\tilde{j}_y(J+\frac{1}{2})\Delta y+\tilde{k}_z(K+\frac{1}{2})\Delta z]} - e^{-j[\tilde{i}_x I\Delta x+\tilde{j}_y(J+\frac{1}{2})\Delta y+\tilde{k}_z(K-\frac{1}{2})\Delta z]}}{e^{-j[\tilde{i}_x I\Delta x+\tilde{j}_y(J+\frac{1}{2})\Delta y+\tilde{k}_z K\Delta z]}\Delta z} - H_{z0}\frac{e^{-j[\tilde{i}_x(I+\frac{1}{2})\Delta x+\tilde{j}_y(J+\frac{1}{2})\Delta y+\tilde{k}_z K\Delta z]} - e^{-j[\tilde{i}_x(I-\frac{1}{2})\Delta x+\tilde{j}_y(J+\frac{1}{2})\Delta y+\tilde{k}_z K\Delta z]}}{e^{-j[\tilde{i}_x I\Delta x+\tilde{j}_y(J+\frac{1}{2})\Delta y+\tilde{k}_z K\Delta z]}\Delta x}\right) \tag{A42}$$

$$\left(\frac{1}{\Delta t}\right)^{\alpha} E_{z0} = \frac{1}{\varepsilon_\alpha z_s}\left(H_{y0}\frac{e^{-j[\tilde{i}_x(I+\frac{1}{2})\Delta x+\tilde{j}_y J\Delta y+\tilde{k}_z(K+\frac{1}{2})\Delta z]} - e^{-j[\tilde{i}_x(I-\frac{1}{2})\Delta x+\tilde{j}_y J\Delta y+\tilde{k}_z(K+\frac{1}{2})\Delta z]}}{e^{-j[\tilde{i}_x I\Delta x+\tilde{j}_y J\Delta y+\tilde{k}_z(K+\frac{1}{2})\Delta z]}\Delta x} - H_{x0}\frac{e^{-j[\tilde{i}_x I\Delta x+\tilde{j}_y(J+\frac{1}{2})\Delta y+\tilde{k}_z(K+\frac{1}{2})\Delta z]} - e^{-j[\tilde{i}_x I\Delta x+\tilde{j}_y(J-\frac{1}{2})\Delta y+\tilde{k}_z(K+\frac{1}{2})\Delta z]}}{e^{-j[\tilde{i}_x I\Delta x+\tilde{j}_y J\Delta y+\tilde{k}_z(K+\frac{1}{2})\Delta z]}\Delta y}\right) \tag{A43}$$

where

$$z_s = \sum_{l=0}^{N} w_l^{\alpha} e^{j\tilde{\omega}(-l+\frac{1}{2})\Delta t}. \tag{A44}$$

The system of Equations (A38)–(A43) can be written in the matrix form

$$\underbrace{\begin{bmatrix} -\mu_\alpha & 0 & 0 & 0 & \delta_z & -\delta_y \\ 0 & -\mu_\alpha & 0 & -\delta_z & 0 & \delta_x \\ 0 & 0 & -\mu_\alpha & \delta_y & -\delta_x & 0 \\ 0 & -\delta_z & \delta_y & -\varepsilon_\alpha & 0 & 0 \\ \delta_z & 0 & -\delta_x & 0 & -\varepsilon_\alpha & 0 \\ -\delta_y & \delta_x & 0 & 0 & 0 & -\varepsilon_\alpha \end{bmatrix}}_{=\mathbf{U}} \begin{bmatrix} H_{x0} \\ H_{y0} \\ H_{z0} \\ E_{x0} \\ E_{y0} \\ E_{z0} \end{bmatrix} = \begin{bmatrix} 0 \\ 0 \\ 0 \\ 0 \\ 0 \\ 0 \end{bmatrix} \tag{A45}$$

where

$$\delta_x = (\Delta t)^{\alpha}\frac{e^{-j[\tilde{i}_x\frac{1}{2}\Delta x]} - e^{j[\tilde{i}_x\frac{1}{2}\Delta x]}}{z_s\Delta x} \tag{A46}$$

$$\delta_y = (\Delta t)^{\alpha} \frac{e^{-j[\tilde{j}_y \frac{1}{2}\Delta y]} - e^{j[\tilde{j}_y \frac{1}{2}\Delta y]}}{z_s \Delta y} \tag{A47}$$

$$\delta_z = (\Delta t)^{\alpha} \frac{e^{-j[\tilde{k}_z \frac{1}{2}\Delta z]} - e^{j[\tilde{k}_z \frac{1}{2}\Delta z]}}{z_s \Delta z}. \tag{A48}$$

The system of Equations (A45) is homogeneous. In order to obtain any nontrivial (nonzero) solution, the determinant of the matrix **U** has to be equal 0. The matrix **U** can be interpreted as the block matrix

$$\mathbf{U} = \begin{bmatrix} \mathbf{A} & \mathbf{B} \\ \mathbf{C} & \mathbf{D} \end{bmatrix} \tag{A49}$$

where **A**, **B**, **C**, **D** are 3×3 matrices. They commute because $\mathbf{B} = -\mathbf{C}$ and $\frac{1}{\mu_\alpha}\mathbf{A} = \frac{1}{\varepsilon_\alpha}\mathbf{D} = -\mathbf{I}$, where **I** is the identity matrix. In such a case, the determinant of matrix **U** can be calculated using the following property [28]:

$$\det(\mathbf{U}) = \det(\mathbf{AD} - \mathbf{BC}). \tag{A50}$$

Hence, one obtains

$$\begin{aligned} \det(\mathbf{U}) &= \det\left(\begin{bmatrix} \mu_\alpha\varepsilon_\alpha - {\delta_y}^2 - {\delta_z}^2 & \delta_x\delta_y & \delta_x\delta_z \\ \delta_x\delta_y & \mu_\alpha\varepsilon_\alpha - {\delta_x}^2 - {\delta_z}^2 & \delta_y\delta_z \\ \delta_x\delta_z & \delta_y\delta_z & \mu_\alpha\varepsilon_\alpha - {\delta_x}^2 - {\delta_y}^2 \end{bmatrix}\right) \\ &= \mu_\alpha\varepsilon_\alpha({\delta_x}^2 + {\delta_y}^2 + {\delta_z}^2 - \mu_\alpha\varepsilon_\alpha)^2. \end{aligned} \tag{A51}$$

Equating the determinant to 0, one obtains

$$\mu_\alpha\varepsilon_\alpha = {\delta_x}^2 + {\delta_y}^2 + {\delta_z}^2. \tag{A52}$$

Using (A11) one obtains

$$\begin{aligned} \left(\frac{e^{j\omega\Delta t\frac{1}{2}}\left(1 - e^{-j\omega\Delta t}\right)^{\alpha}}{2j}\right)^2 &= \left((\Delta t)^{\alpha}\frac{e^{-j[\tilde{i}_x\frac{1}{2}\Delta x]} - e^{j[\tilde{i}_x\frac{1}{2}\Delta x]}}{2j\sqrt{\mu_\alpha\varepsilon_\alpha}\Delta x}\right)^2 + \\ \left((\Delta t)^{\alpha}\frac{e^{-j[\tilde{j}_y\frac{1}{2}\Delta y]} - e^{j[\tilde{j}_y\frac{1}{2}\Delta y]}}{2j\sqrt{\mu_\alpha\varepsilon_\alpha}\Delta y}\right)^2 &+ \left((\Delta t)^{\alpha}\frac{e^{-j[\tilde{k}_z\frac{1}{2}\Delta z]} - e^{j[\tilde{k}_z\frac{1}{2}\Delta z]}}{2j\sqrt{\mu_\alpha\varepsilon_\alpha}\Delta z}\right)^2. \end{aligned} \tag{A53}$$

From (A53), one directly obtains the numerical-dispersion relation for the three-dimensional FO FDTD algorithm

$$\begin{aligned} \left(\frac{e^{j\omega\Delta t\frac{1}{2}}\left(1 - e^{-j\omega\Delta t}\right)^{\alpha}}{2j}\right)^2 &= \frac{(\Delta t)^{2\alpha}}{\mu_\alpha\varepsilon_\alpha(\Delta x)^2}\left[\sin\left(\frac{\tilde{i}_x\Delta x}{2}\right)\right]^2 + \\ \frac{(\Delta t)^{2\alpha}}{\mu_\alpha\varepsilon_\alpha(\Delta y)^2}\left[\sin\left(\frac{\tilde{j}_y\Delta y}{2}\right)\right]^2 &+ \frac{(\Delta t)^{2\alpha}}{\mu_\alpha\varepsilon_\alpha(\Delta z)^2}\left[\sin\left(\frac{\tilde{k}_z\Delta z}{2}\right)\right]^2. \end{aligned} \tag{A54}$$

If one omits the x- and y-related terms in (A54), it simplifies that formula to the one-dimensional case (A12). Substituting

$$\begin{aligned} \xi_\alpha = \Bigg(\frac{(\Delta t)^{2\alpha}}{\mu_\alpha\varepsilon_\alpha(\Delta x)^2}\left[\sin\left(\frac{\tilde{i}_x\Delta x}{2}\right)\right]^2 + \frac{(\Delta t)^{2\alpha}}{\mu_\alpha\varepsilon_\alpha(\Delta y)^2}\left[\sin\left(\frac{\tilde{j}_y\Delta y}{2}\right)\right]^2 + \\ \frac{(\Delta t)^{2\alpha}}{\mu_\alpha\varepsilon_\alpha(\Delta z)^2}\left[\sin\left(\frac{\tilde{k}_z\Delta z}{2}\right)\right]^2\Bigg)^{\frac{1}{2\alpha}} \end{aligned} \tag{A55}$$

into (A54), and continuing as in the one-dimensional case, one obtains

$$2^{\frac{1}{\alpha}}\left(\frac{(\Delta t)^{2\alpha}}{\mu_\alpha \varepsilon_\alpha (\Delta x)^2}\left[\sin\left(\frac{\tilde{i}_x \Delta x}{2}\right)\right]^2+\frac{(\Delta t)^{2\alpha}}{\mu_\alpha \varepsilon_\alpha (\Delta y)^2}\left[\sin\left(\frac{\tilde{j}_y \Delta y}{2}\right)\right]^2+\frac{(\Delta t)^{2\alpha}}{\mu_\alpha \varepsilon_\alpha (\Delta z)^2}\left[\sin\left(\frac{\tilde{k}_z \Delta z}{2}\right)\right]^2\right)^{\frac{1}{2\alpha}} \leq 2. \tag{A56}$$

After assuming the maximum possible values of the sine functions, one obtains the stability condition for the three-dimensional FO FDTD algorithm

$$\Delta t \leq 2^{1-\frac{1}{\alpha}}\left(\frac{\sqrt{\mu_\alpha \varepsilon_\alpha}}{\sqrt{\frac{1}{(\Delta x)^2}+\frac{1}{(\Delta y)^2}+\frac{1}{(\Delta z)^2}}}\right)^{\frac{1}{\alpha}}. \tag{A57}$$

After omitting terms related to the x- and y-dimensions, this stability condition simplifies to the one-dimensional condition (A29). Taking $\alpha = 1$, one obtains the stability condition for IO FDTD

$$\Delta t \leq \frac{\sqrt{\mu_0 \varepsilon_0}}{\sqrt{\frac{1}{(\Delta x)^2}+\frac{1}{(\Delta y)^2}+\frac{1}{(\Delta z)^2}}}. \tag{A58}$$

References

1. Nasrolahpour, H. A Note on Fractional Electrodynamics. *Commun. Nonlinear Sci. Numer. Simul.* **2013**, *18*, 2589–2593. [CrossRef]
2. Tarasov, V.E. *Fractional Dynamics: Applications of Fractional Calculus to Dynamics of Particles, Fields and Media*; Springer Science & Business Media: Berlin/Heidelberg, Germany, 2011.
3. Gabriel, S.; Lau, R.W.; Gabriel, C. The Dielectric Properties of Biological Tissues: III. Parametric Models for the Dielectric Spectrum of Tissues. *Phys. Med. Biol.* **1996**, *41*, 2271. [CrossRef] [PubMed]
4. Westerlund, S. Dead Matter Has Memory! *Phys. Scr.* **1991**, *43*, 174. [CrossRef]
5. Westerlund, S.; Ekstam, L. Capacitor Theory. *IEEE Trans. Dielectr. Electr. Insul.* **1994**, *1*, 826–839. [CrossRef]
6. Engheta, N. Fractional Curl Operator in Electromagnetics. *Microw. Opt. Technol. Lett.* **1998**, *17*, 86–91. [CrossRef]
7. Naqvi, S.; Naqvi, Q.; Hussain, A. Modelling of Transmission Through a Chiral Slab Using Fractional Curl Operator. *Opt. Commun.* **2006**, *266*, 404–406. [CrossRef]
8. Engheta, N. On the Role of Fractional Calculus in Electromagnetic Theory. *IEEE Antennas Propag. Mag.* **1997**, *39*, 35–46. [CrossRef]
9. Taflove, A.; Hagness, S.C. *Computational Electrodynamics: The Finite-Difference Time-Domain Method*, 3rd ed.; Artech House: Norwood, Australia, 2005.
10. Mescia, L.; Bia, P.; Caratelli, D. FDTD-Based Electromagnetic Modeling of Dielectric Materials with Fractional Dispersive Response. *Electronics* **2022**, *11*, 1588. [CrossRef]
11. Kelley, D.F.; Destan, T.J.; Luebbers, R.J. Debye Function Expansions of Complex Permittivity Using a Hybrid Particle Swarm-Least Squares Optimization Approach. *IEEE Trans. Antennas Propag.* **2007**, *55*, 1999–2005. [CrossRef]
12. Wuren, T.; Takai, T.; Fujii, M.; Sakagami, I. Effective 2-Debye-Pole FDTD Model of Electromagnetic Interaction Between Whole Human Body and UWB Radiation. *IEEE Microw. Wirel. Components Lett.* **2007**, *17*, 483–485. [CrossRef]
13. Causley, M.F.; Petropoulos, P.G.; Jiang, S. Incorporating the Havriliak–Negami Dielectric Model in the FD-TD Method. *J. Comput. Phys.* **2011**, *230*, 3884–3899. [CrossRef]
14. Su, S.; Dai, W.; Haynie, D.T.; Simicevic, N. Use of the Z-Transform to Investigate Nanopulse Penetration of Biological Matter. *Bioelectromagnetics* **2005**, *26*, 389–397. [CrossRef] [PubMed]
15. Guo, B.; Li, J.; Zmuda, H. A New FDTD Formulation for Wave Propagation in Biological Media with Cole–Cole Model. *IEEE Microw. Wirel. Compon. Lett.* **2006**, *16*, 633–635. [CrossRef]
16. Chakarothai, J. Novel FDTD Scheme for Analysis of Frequency-Dependent Medium Using Fast Inverse Laplace Transform and Prony's Method. *IEEE Trans. Antennas Propag.* **2019**, *67*, 6076–6089. [CrossRef]
17. Rekanos, I.T.; Papadopoulos, T.G. An Auxiliary Differential Equation Method for FDTD Modeling of Wave Propagation in Cole-Cole Dispersive Media. *IEEE Trans. Antennas Propag.* **2010**, *58*, 3666–3674. [CrossRef]
18. Abdullah, H.H.; Elsadek, H.; ElDeeb, H.; Bagherzadeh, N. Fractional Derivatives Based Scheme for FDTD Modeling of n th-Order Cole–Cole Dispersive Media. *IEEE Antennas Wirel. Propag. Lett.* **2012**, *11*, 281–284. [CrossRef]
19. Mescia, L.; Bia, P.; Caratelli, D. Fractional-Calculus-Based FDTD Method for Solving Pulse Propagation Problems. In Proceedings of the 2015 International Conference on Electromagnetics in Advanced Applications (ICEAA), Turin, Italy, 7–11 September 2015; IEEE: Piscataway, NJ, USA, 2015; pp. 460–463.

20. Mescia, L.; Bia, P.; Caratelli, D. Fractional-Calculus-Based Electromagnetic Tool to Study Pulse Propagation in Arbitrary Dispersive Dielectrics. *Phys. Status Solidi (A)* **2019**, *216*, 1800557. [CrossRef]
21. Moreles, M.A.; Lainez, R. Mathematical Modelling of Fractional Order Circuit Elements and Bioimpedance Applications. *Commun. Nonlinear Sci. Numer. Simul.* **2017**, *46*, 81–88. [CrossRef]
22. Stefański, T.P.; Gulgowski, J. Signal Propagation in Electromagnetic Media Described by Fractional-Order Models. *Commun. Nonlinear Sci. Numer. Simul.* **2020**, *82*, 105029. [CrossRef]
23. Stefański, T.P.; Gulgowski, J. Fundamental Properties of Solutions to Fractional-Order Maxwell's Equations. *J. Electromagn. Waves Appl.* **2020**, *34*, 1955–1976. [CrossRef]
24. Li, C.; Zeng, F. *Numerical Methods for Fractional Calculus*; CRC Press: Boca Raton, FL, USA, 2015; Volume 24.
25. Gulgowski, J.; Stefański, T.P.; Trofimowicz, D. On Applications of Elements Modelled by Fractional Derivatives in Circuit Theory. *Energies* **2020**, *13*, 5768. [CrossRef]
26. Luchko, Y.; Mainardi, F.; Povstenko, Y. Propagation Speed of the Maximum of the Fundamental Solution to the Fractional Diffusion–Wave Equation. *Comput. Math. Appl.* **2013**, *66*, 774–784. [CrossRef]
27. Yuste, S.B.; Acedo, L. An Explicit Finite Difference Method and a New von Neumann-Type Stability Analysis for Fractional Diffusion Equations. *SIAM J. Numer. Anal.* **2005**, *42*, 1862–1874. [CrossRef]
28. Silvester, J.R. Determinants of Block Matrices. *Math. Gaz.* **2000**, *84*, 460–467. [CrossRef]